Physics – Uspekhi **65** (11) 1139 – 1154 (2022)

CONFERENCES AND SYMPOSIA

PACS numbers: 82.30.Vy, 92.30.Np, 92.70.Mn

FORUM 'USPEKHI-2021': CLIMATE CHANGE AND GLOBAL ENERGY ISSUES
(Joint Scientific session of the Physical Sciences Division, Chemistry and Materials Sciences Division,
Division of Earth Sciences and Division of Energetics, Machinery, Mechanical Engineering
and Control Processes of the Russian Academy of Sciences, January 19, 2021)

Catalytic methods of converting carbon dioxide into useful products to reduce the impact of coal generation on global climate change

Z R Ismagilov, E V Matus, L Li

DOI: https://doi.org/10.3367/UFNe.2021.07.039084

Contents

Abstract. **Coal generation is one of the main sources of carbon dioxide emissions and makes a significant contribution to global climate change. In general, to curb global warming and to transition to a carbon-neutral economy, it is urgent to develop and improve methods for capturing and utilizing carbon dioxide. The most promising processing methods are those of catalytic conversion of CO_2 into valuable chemical products. This article discusses methods of CO_2 utilization, including synthesis reactions of low-molecular compounds ($HCOOH$, CO, H_2CO, CH_3OH, CH_4) and reactions to obtain high-molecular organic substances (carbamates $RR'NCOOR''$, carbonates $(RO)_2CO$, carboxylates $RCOOH$). The results of research on the creation of a number of effective nanosized catalysts for these processes are presented.**

Keywords: coal generation, climate, carbon dioxide, CO_2 conversion, catalysis, chemical products

1. Introduction

Carbon dioxide (CO_2), produced when burning fossil fuels, (coal, oil, and natural gas) is one of the main greenhouse gases. At present, the technogenic emission of carbon dioxide into the atmosphere is still high and amounts on average to 34 billion tons per year [1, 2]. In terms of CO_2 emissions, Russia ranks fourth in the world (1.7 billion tons per year) after China (10.1 billion tons per year), the USA (5.4 billion tons per year), and India (2.7 billion tons per year).

During the last 200 years, CO_2 concentration in the atmosphere increased from 270 to 418 ppm, mainly because of the continuous consumption of fossil fuels: $\sim$ 22 million tons of coal, $\sim$ 12 million tons of oil, and $\sim$ 10 billion m^3 of natural gas daily [3, 4]. At the current stage of the world's economy, coal, oil, and natural gas remain the dominant energy sources, providing up to 80% of total energy needs. Accordingly, consumers of primary energy resources — thermal power plants and transport — are the main sources of deterioration of the ecological state of the environment and climate change. The contribution to carbon dioxide emissions from burning fuel is distributed as follows: coal — 44%, oil — 33%, natural gas — 23%. It should be noted that the burning of coal at a thermal power plant results in the emission of 0.34 kg of carbon dioxide per kilowatt-hour of electricity, which is 1.5 times more than when burning natural gas (Fig. 1) [5].

Coal has been for many decades and will remain in the nearest future one of the cheapest and most easily available energy sources [6]. At present, the proportion of coal-burning generation in the rated capacity of electric power plants in Russia is about 22% (56.6 GW). In the Siberian Federal District, the proportion of coal generation attains 65%, and in the Far Eastern Federal District, 93%. Russia ranks 13th in

---

Z R Ismagilov [1, 2, *], **E V Matus** [2, **], **L Li** [3, ***]
(1) Federal Research Center for Coal and Coal Chemistry,
Siberian Branch of the Russian Academy of Sciences,
prosp. Sovetskii 18, 650000 Kemerovo, Russian Federation
(2) Federal Research Center Boreskov Institute of Catalysis,
Siberian Branch of the Russian Academy of Science,
prosp. Academika Lavrent'eva 5, 630090 Novosibirsk,
Russian Federation
(3) Institute of Coal Chemistry, Chinese Academy of Sciences,
27th South Taoyuan Road, Taiyuan, Shanxi, P.R. China
E-mail: (*) zinfer1@mail.ru, (**) matus@catalysis.ru, (***) lilei@sxicc.ac.cn

Received 23 May 2021
Uspekhi Fizicheskikh Nauk **192** (11) 1214 – 1230 (2022)
Translated by V L Derbov

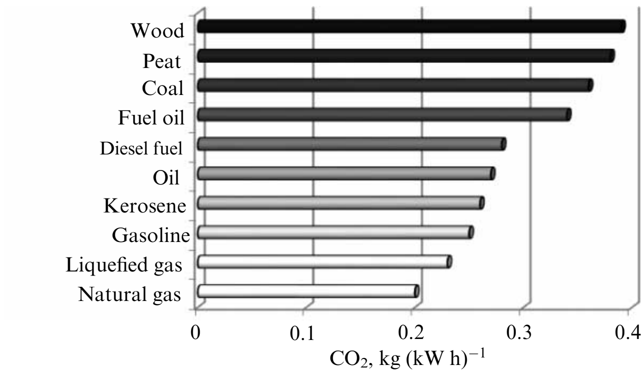

Figure 1. Amount of carbon dioxide released per kW h of electricity produced by burning various types of fuel (according to [5]).

the world in terms of the amount of energy generated by coal thermal and power stations, after China, India, the USA, EC, and other states whose energy systems are largely based on coal-burning generation [7].

The process of fuel combustion is a complex phenomenon, including a few hundred elementary chemical reactions (as a simple example, we present below some radical reactions of the methane oxidation process (1)–(7)); considering mass and heat transport processes is additionally required. The character of transformation of organic fuel molecules is determined by the conditions of the process. A high temperature of combustion, increased concentration of oxygen, and optimization of the process parameters allow avoiding the formation of high-molecular-weight compounds, including highly toxic polycyclic aromatic hydrocarbons and soot [8]. The multistage process of oxidative destruction of fuel molecules is accompanied by the formation of carbon oxides: CO and the final product of combustion, carbon dioxide CO$_2$:

$$CH_4 + OH^\bullet \rightarrow CH_3^\bullet + H_2O\,, \tag{1}$$

$$CH_3^\bullet + O_2 \rightarrow CH_3O_2^\bullet\,, \tag{2}$$

$$CH_3O_2^\bullet \rightarrow HCHO + HO^\bullet\,, \tag{3}$$

$$HCHO + OH^\bullet \rightarrow H_2O + HCO^\bullet\,, \tag{4}$$

$$HCO^\bullet + O_2 \rightarrow CO + HO_2^\bullet\,, \tag{5}$$

$$CO + OH^\bullet \rightarrow CO_2 + H^\bullet\,, \tag{6}$$

$$CH_3^\bullet + CH_3^\bullet \rightarrow C_2H_6 \ldots \rightarrow C_2H_5^\bullet + CH_3^\bullet \rightarrow C_3H_8 \ldots \tag{7}$$

The specific amount of CO$_2$ produced in the course of fuel-burning electric energy generation depends on the carbon content in the fuel and can be calculated using the formula [9]

$$q_{CO_2} = \frac{c_f}{h_f}\,\frac{M_{CO_2}}{M_C}\,,$$

where q_{CO_2} is the specific emission of CO$_2$ [kg (kW h)$^{-1}$], c_f is the specific content of carbon in the fuel (C [kg] per kg of fuel), h_f is the specific energy content in the fuel (kW h per kg of fuel), M_C is the molecular weight of carbon (kg kmol^{-1}], and M_{CO_2} is the molecular weight of carbon dioxide [kg kmol^{-1}].

The heat content or the amount of energy produced upon burning fuel is mainly determined by the content of carbon and hydrogen in it, whose combustion heat is 34.4 and 120.5 MJ kg^{-1}, respectively. According to thermodynamic data for the reactions of burning coal,

$$C + O_2 \rightarrow CO_2\,, \qquad 394\ \text{kJ per mol } CO_2\,, \tag{8}$$

petrol

$$2C_8H_{18} + O_2 \rightarrow 16CO_2 + 18H_2O\,, \qquad 635\ \text{kJ per mol } CO_2\,, \tag{9}$$

and natural gas

$$CH_4 + O_2 \rightarrow CO_2 + 2H_2O\,, \qquad 803\ \text{kJ per mol } CO_2\,, \tag{10}$$

the amount of energy obtained per mole of emitted carbon dioxide increases with the growth of the hydrogen/carbon ratio in the fuel.

Water and various elements such as sulphur and nonflammable elements in some kinds of fuel reduce the fuel heating power and increase the content of CO$_2$ per unit of produced energy.

Since 2010, a decrease has been observed in the global carbon capacity of electric energy (the amount of CO$_2$ emissions per unit of electric energy produced). This is due to an increase in the contribution to the energy production structure from renewable energy sources, gas generation, extended use of steam-gas power units, as well as coal power units with high and ultrahigh steam parameters. The carbon capacity of electric energy in different countries in the world varies within wide limits (50–800 g CO$_2$ per kW h) and is determined by the structure of electric energy production. For example, in France, this indicator is low (52 g of CO$_2$ per kW h), which is due to the prevalence of atomic energy in the country. The high values of the carbon capacity indicator in the USA (433 g of CO$_2$ per kW h), Germany (447 g of CO$_2$ per kW h), and China (627 g of CO$_2$ per kW h) are caused by the substantial proportion of coal in the production of electric energy — 31, 42, and 68%, respectively [10]. The carbon capacity of electric energy in Russia (358 g of CO$_2$ per kW h) is lower than the world mean value (480 g of CO$_2$ per kW h), which is explained by the high proportion of natural gas (48%), atomic energy (18%), and hydro energy (17%) in electric power production [10].

The presence of greenhouse gases in the atmosphere affects the energy balance on Earth's surface, formed by the absorption of the solar radiation flux in the visible spectrum, on the one hand, and emission in the infrared range, on the other hand. The energy absorption/emission mechanism is determined by transitions between vibration-rotational energy levels in molecules of atmospheric gases.

Carbon dioxide is recognized as a significant climate regulator on the globe — the growing greenhouse effect is associated with an increase in CO$_2$ concentration. This is determined by the specific features of energy absorption by the CO$_2$ molecule in the infrared spectrum [11, 12]. In the case of CO$_2$, the atmospheric transparency is determined by two bands: valence antisymmetric vibration in the region of 2200–2400 cm^{-1} and bending vibration in the region of 500–900 cm^{-1}. The second band is of great importance, since it falls into the region of maximum radiation of bodies at near-room temperature. The absorption of light by the CO$_2$ molecule falls at the maximum intensity of infrared radiation, which significantly affects the shape of the spectrum of outgoing light and, accordingly, the energy balance of the planet. With an increase in CO_2 concentration, the CO_2 absorption band becomes broader and deeper, and, therefore, a reduction in the atmospheric transparency window for infrared radiation is observed. In this case, the energy flux leaving Earth reduces, and, therefore, the global temperature grows.

The contribution of each gas to the greenhouse effect is determined by the gas's molecular characteristics, its prevalence in the atmosphere, and other indirect effects which it can manifest. For example, the direct radiative effect of a unit mass of methane by nearly 70–84 times exceeds that of carbon dioxide during a 20-year period, but methane is present in lower concentrations and has a shorter lifetime in the atmosphere than does carbon dioxide. As a result, with the growth of CO_2 anthropogenic emissions and considering the global warming potential (GWP), the real contribution of carbon dioxide to the greenhouse effect is a significant regulator of climatic changes.

In accordance with the UN Framework Convention on Climate Change, the Paris Agreement came into force in 2016, which regulates the measures of the international community to reduce the amount of carbon dioxide in the atmosphere and, accordingly, the rate of global warming. The participant countries in the Paris Agreement undertake to adopt national plans to reduce greenhouse gas emissions, develop national strategies for the transition to a carbon-neutral economy, and establish an international exchange of 'green' technologies in the field of energy efficiency, industry, and construction. Monitoring the carbon footprint will be the main tool for influencing the global economy in the transition to the decarbonization regime. In particular, according to the Paris Agreement, the emission of greenhouse gases in Russia till 2030 should amount to no more than 70% of the 1990 level.

Three main stages of the strategy for reducing carbon dioxide content in the atmosphere are considered: a reduction in the produced CO_2 amount, carbon capture and storage (CCS), and carbon capture and utilization (CCU) (Fig. 2) [13, 14].

The first stage of this strategy implies reducing the use of fossil fuels by moving to energy sources and synthetic chemical compounds obtained using solar or wind energy. It is expected that ecologically pure energy effective technologies in the fuel-energy complex, industry, and transport will be introduced to reduce the generation and consumption of power and, respectively, to reduce carbon dioxide emission [15].

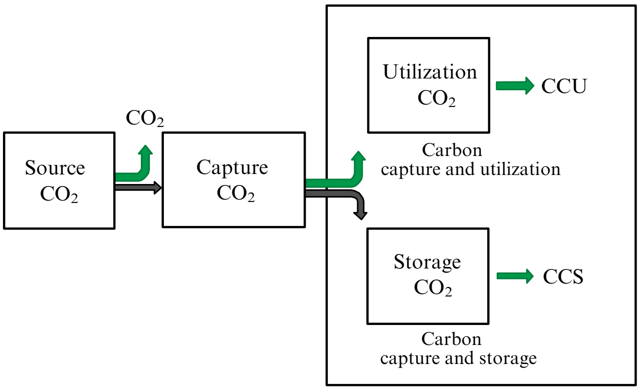

Figure 2. Strategies for reducing CO_2 anthropogenic emissions [14].

Table 1. Types of CO_2 adsorbents and their main characteristics [21].

Adsorbent type	Adsorption conditions	CO_2 capacity [mmol] per g
Low-temperature adsorbents		
Carbon materials	$\leqslant 80\,°C$, 1 atm	$\leqslant 3.5$
Zeolites	$\leqslant 100\,°C$, 1 atm	$\leqslant 4.9$
Metal-Organic Frameworks, MOF	$\leqslant 100\,°C$, 1 atm	$\leqslant 4.5$
Alkali metal carbonates	$\leqslant 120\,°C$, 1 atm	$\leqslant 9.4$
Amine-containing sorbents	$\leqslant 60\,°C$, 1 atm	$\leqslant 5.5$
Medium-temperature adsorbents		
Layered double hydroxides	$200-400\,°C$	$\leqslant 1.4$
High-temperature adsorbents		
CaO-based adsorbents	$600-700\,°C$	$\leqslant 11.6$
Ceramic sorbents containing alkali metals	$500-600\,°C$	$\leqslant 6.5$

Capture and storage of carbon dioxide includes the separation of CO_2 from emissions from coal-fired power plants and industrial enterprises, transportation, and long-term isolation from the atmosphere by storage in deep-lying geological formations (for example, exhausted oil and gas-bearing strata) or industrial fixation of CO_2 as part of inorganic carbonates [16]. There are several commercial-scale carbon dioxide conservation projects currently underway. For example, oil and natural gas production at the Sleipnir oil and gas field on the Norwegian continental shelf is accompanied by the injection of CO_2 (about 1 million tons per year) into a geological structure called the Utsira formation, which is a layer of porous sandstone.

Sorption methods of carbon dioxide gas capture and concentration are rather attractive because of their low cost and the simplicity of technical implementation. Various types of CO_2 adsorbents are proposed differing in chemical composition, texture, morphology, and, correspondingly, capacity and selectivity [17–20]. Conventionally, sorbents can be divided into three big groups depending on the range of their working temperature: low-, middle-, and high-temperature adsorbents with the sorption/desorption temperature $T < 200\,°C$, $200 < T < 400\,°C$, and $T > 400\,°C$, respectively [21]. Table 1 presents their main characteristics.

After capture and concentration, CO_2 can serve as an initial reagent for the synthesis of many chemical products (Fig. 3) [22]. Modern technologies of CO_2 reprocessing into valuable products are at various levels of achievement — industrial processes, pilot projects, and laboratory developments.

From a sustainable development point of view, the chemical processing of carbon dioxide is feasible, provided that all other chemicals that serve as reagents or catalysts come from environmentally friendly sources. Currently, the annual volume of industrial utilization of carbon dioxide is about 120 million tons (Table 2) [3], which still does not exceed 0.5% of total anthropogenic CO_2 emissions. In this regard, the expansion of the scope of CO_2 application as an initial reagent for chemical processes is a very topical issue aimed at solving the problems of environmental safety and rational nature management [23–25].

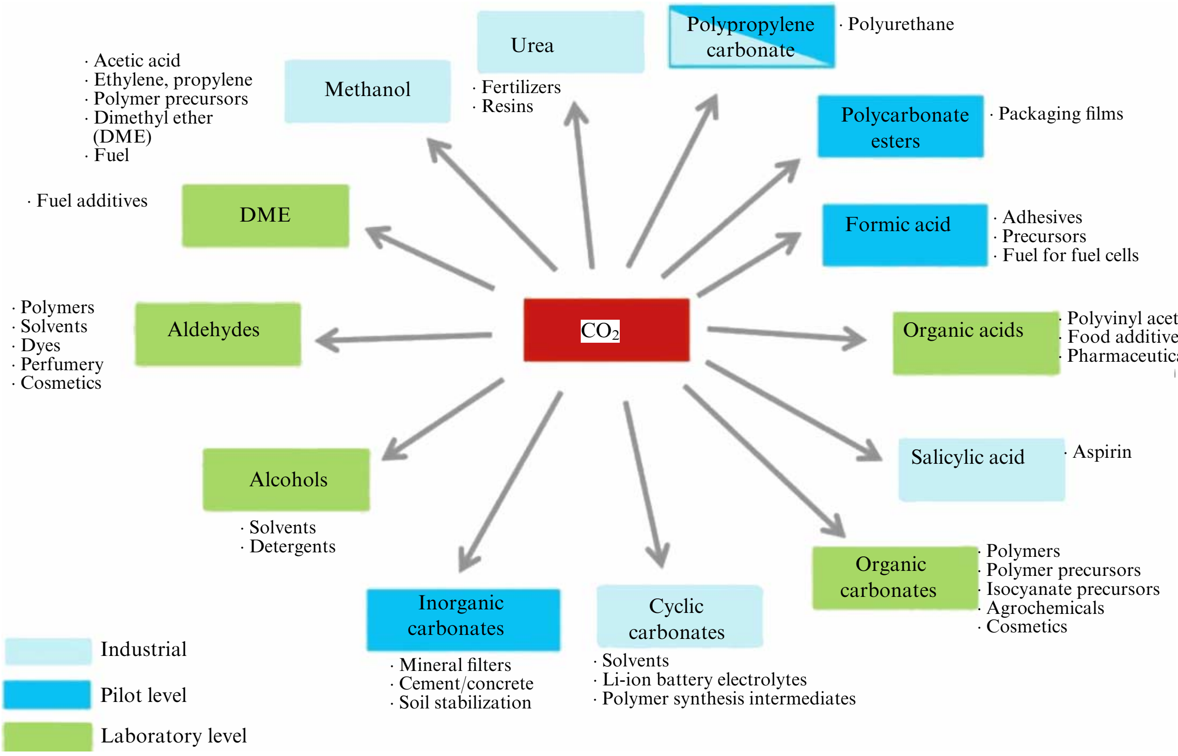

Figure 3. Products obtained from CO_2 processing [22].

Table 2. Amounts of CO_2 use (according to [3]).

Field of application	Amount, 10^6 t year^{-1}
Chemical industry	114.22
— urea	70
— methanol	14
— inorganic carbonates	30
— organic carbonates	0.2
— salicylic acid	0.02
Technology	10
Food industry	8

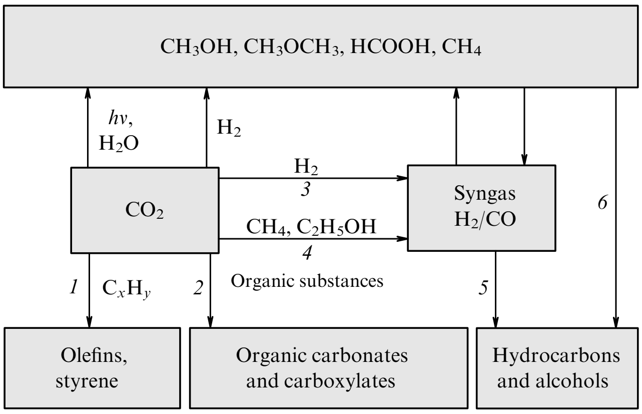

Figure 4. Main ways of processing CO_2 into basic chemical products: *1* — oxidative dehydrogenation; *2* — synthesis of macromolecular compounds and polymers; *3* — reverse reaction with respect to the conversion of CO with water vapor; *4* — carbon dioxide conversion of methane (ethanol); *5* — Fischer–Tropsch synthesis; *6* — synthesis of higher alcohols and hydrocarbons from low molecular weight compounds.

The processes of CO_2 catalytic conversion include its interaction with hydrogen and hydrocarbons, as well as reactions in which CO_2 plays the role of an oxidant (Table 3) [26]. It should be noted that, for carbon dioxide reprocessing by its reduction with the formation of methanol, dimethyl ether, methane, and other hydrocarbons via the Fisher–Tropsch reaction, it is necessary to solve the problem of clean hydrogen production, i.e., its production without CO_2 emission.

In this paper, we present a brief analysis of literature data on prospective methods for catalytic conversion of CO_2 into valuable chemical products, as well as results of studies on creating efficient nanocatalysts for these processes.

2. Studies of catalysts and catalytic reactions of carbon dioxide. Overview of industrial processes for converting CO_2 into value-added chemicals

The general path of CO_2 chemical utilization is its catalytic conversion into chemical compounds in demand in various branches of industry and production of a wide range of consumer goods. Catalysis is a key technology for the efficient and sustainable use of resources, waste reduction, and pollution reduction, and is critical to the economies of many countries. Catalysts are used in nearly 90% of all chemical processes, including oil refining, oil chemistry, gas chemistry, and the production of polymers and fertilizers. The contribution of these processes provides up to 30–40% of the world's gross domestic product. Heterogeneous catalysts are a key component of most processes from oil chemistry production to catalytic convertors of exhaust gases in combustion engines.

The use of CO_2 in the chemical industry has a number of advantages, such as nontoxicity, low cost, availability, renewability, and nonflammability [27, 28]. Figure 4 presents the main paths of CO_2 conversion into basic chemical products.

Table 3. Main processes of CO_2 catalytic conversion [26].

Process	Reaction	Product	Catalyst type
	$CO_2 + H_2$		
Methanol synthesis	$CO_2 + 3H_2 \rightarrow CH_3OH + H_2O$	CH_3OH	Cu, Pd, Ru, Cu/Zn, Mo_2C, MoS_2, In_2O_3
Dimethyl ether synthesis	$2CO_2 + 6H_2 \rightarrow CH_3OCH_3 + 3H_2O$	CH_3OCH_3	Cu/Zn/HZSM-5, Pd(Ga)/ZSM-5, Cu/Fe/Zr/HZSM-5
Formic acid synthesis	$CO_2 + H_2 \rightarrow HCOOH$	HCOOH	Supported catalysts Ru, Ir, Au, Ni, Pd
Methane synthesis	$CO_2 + 4H_2 \rightarrow CH_4 + 2H_2O$	CH_4	Supported or bulk catalysts N, Ru, Rh, Pd, Cu, Mo_2C, MoS_2
Fischer–Tropsch synthesis	$nCO_2 + (3n+1)H_2 \rightarrow C_nH_{2n+2} + 2nH_2O$	Alkanes	Supported or bulk catalysts Fe, Co, Ru, Mo_2C, MoS_2
	$nCO_2 + 3nH_2 \rightarrow C_nH_{2n} + 2nH_2O$	Alkenes	
	CO_2 + hydrocarbon		
Carbon dioxide conversion of methane	$CO_2 + CH_4 \rightarrow 2CO + 2H_2$	Syngas	Supported catalysts Ni, P, Co, Rh, Ru, Mo
Alkane carboxylation	$CO_2 + C_nH_{2n+2} \rightarrow C_nH_{2n+1}COOH$	Carboxylic acids	Zn/ZSM-5, supported catalysts Cu/Co, Rh, Pd
Olefin carboxylation	$CO_2 + C_2H_4 \rightarrow C_2H_3COOH$	Acrylic acid	Complexes Ni, W, Mo
Alkyne carboxylation	$CO_2 + C_2H_2 \rightarrow C_2HCOOH$	Propiolic acid	Complexes Ni, Cu
Aromatic carboxylation	$CO_2 + C_6H_6 \rightarrow C_6H_5COOH$	Benzoic acid	Complexes Ni, Cu, Rh, Al/$AlCl_3$
	CO_2 as an oxidizing agent		
Oxidative dehydrogenation	$CO_2 + C_nH_{2n+2} \rightarrow CO + C_nH_{2n} + H_2O$	Alkenes	Supported catalysts Cr, Fe, Au, V, Ce
Benzene oxidation	$CO_2 + C_6H_6 \rightarrow C_6H_5OH + CO$	Phenol	Mesoporous graphite-like carbon nitride

CO_2 has an ionization potential of 13.73 eV and electron affinity of 3.8 eV, which determines its donor-acceptor properties. The carbon dioxide molecule is highly stable (bond length of 0.116 nm, bond dissociation energy of 1072 kJ mol^{-1}, standard Gibbs energy of formation $\Delta G_f^0 = -396$ kJ mol^{-1}); therefore, its activation requires substantial energy. The use of catalysts capable of efficient and selective CO_2 molecule activation provides a reduction in the activation energy and chemical transformation of carbon dioxide in the desired direction.

The energy profile of a reaction will be determined by the character of change in the degree of carbon oxidation [29]. In accordance with this principle, low- and high-energy reactions are distinguished, in the products of which the carbon atom has an oxidation level of $+2$ and $+4/+3$, respectively. The first group includes, as a rule, endothermic reactions of the synthesis of low-molecular-weight compounds (HCOOH, CO, H_2CO, CH_3OH, CH_4), the second group includes exothermic reactions of the synthesis of high-molecular-weight organic substances (carbamates RR′NNCOOR″N, carbonates $(RO)_2CO$, carboxylates RCOOH).

Currently, CO_2 is used on an industrial scale for the production of the following chemicals [30]:

- carbamide,

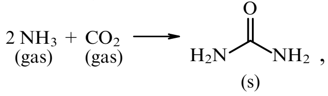

$$\underset{(gas)}{2NH_3} + \underset{(gas)}{CO_2} \longrightarrow \underset{(s)}{H_2N\text{–}C(=O)\text{–}NH_2}, \qquad (11)$$

a standard enthalpy change in the chemical reaction $\Delta H_r^0 = -101$ kJ mol^{-1}, in industry since 1922;

- salicylic acid,

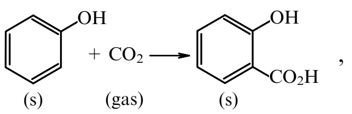

(12)

$\Delta H_r^0 = -31$ kJ mol^{-1}, in industry since 1890;

- ethylene carbonate,

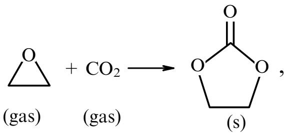

(13)

$\Delta H_r^0 = -144$ kJ mol^{-1}, in industry since the 1950s;

- methanol,

$$\underset{(gas)}{CO_2} + \underset{(gas)}{3H_2} \longrightarrow \underset{(l)}{CH_3OH} + \underset{(l)}{H_2O}, \qquad (14)$$

$\Delta H_r^0 = -130$ kJ mol^{-1}, in industry since 2011.

It is expected that in 2050 the volume of CO_2 conversion into chemicals (carbamide, polycarbonates) and fuels (methanol, methane, dimethyl ether, products of Fisher–Tropsch synthesis) will reach 0.3–0.6 and 1–4.2 billion tons of CO_2 per year, respectively, i.e., will amount to 4–14% of the current level of anthropogenic CO_2 emissions of 34 billion tons per year [2]. To increase the energy efficiency, extend the list, and reduce the cost of producing useful products from CO_2, it is necessary to improve the catalysts and catalytic technologies.

2.1 Synthesis of low-molecular-weight compounds

Currently, a wide range of lower hydrocarbons and their derivatives, which are in demand in the chemical industry, are obtained from nonrenewable natural resources. Within the framework of the concept of sustainable development, alternative methods for the synthesis of such products using CO_2 are being developed, which reduces society's dependence on fossil fuels.

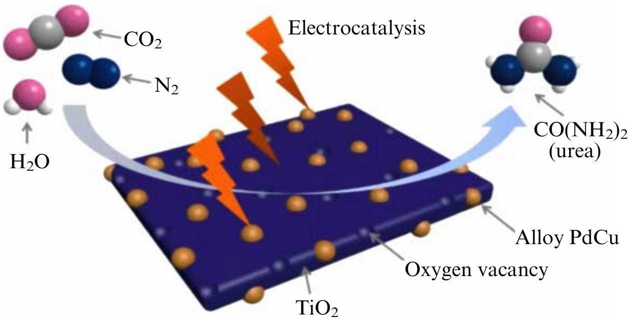

Figure 5. Electrocatalytic synthesis of urea from nitrogen, carbon dioxide, and water at room temperature [35].

2.1.1 Carbamide. By the end of 1972, the capacity of carbamide production plants in the USSR exceeded 5 million tons per year and accounted for more than 30% of world output. In the 1970s, by a government decision, sets of equipment for carbamide production units with a capacity of 330 and 450 thousand tons per year using the technologies of all leading foreign companies were purchased. Ammonia and carbon dioxide are converted to carbamide through ammonium carbamate at a pressure of about 140 bar and a temperature of 180–185 °C. The conversion attains 41% for ammonia and 60% for carbon dioxide. Unreacted ammonia and carbon dioxide enter a stripper, while CO_2 acts as a stripping agent. After condensation, CO_2 and ammonia are recycled and returned to the synthesis process. The heat of condensation is used to generate steam for the CO_2 compressor.

Throughout the world, there are more than five perfect technologies (Stamicarbon, etc.) for carbamide production. One of the new technologies, Urea 2000plus, is successfully used in carbamide production with a capacity of 2700 tons per day in China (China National Offshore Oil Corporation, CNOOC), launched in 2004, as well as in production with a capacity of 3200 tons per day in Qatar (Qafco IV), launched in 2005. At the moment, the development of mega-plants for the production of carbamide with a capacity of up to 5,000 tons per day is also underway. New energy-saving technologies are used to produce carbamide at the gas chemical plant of Gazprom Neftekhim Salavat LLC [31].

In Veliky Novgorod, in 2018, a new unit, Karbamid-600, for carbamide production with a capacity of 600 tons per day was put into operation [32]. The new production facility is based on using the URECON® 2006 technology. Currently, the public joint-stock company (PJSC) Akron is modernizing production, which will increase the capacity from 600 to 2050 tons per day [33]. Investments in the project will amount to 85 million dollars. After the completion of the project in 2021, the total annual urea production capacity will increase by 0.5 million tons to reach 1.9 million tons, which will make Akron the largest carbamide production site, not only in Russia, but also in Europe.

The use of carbon dioxide in carbamide production has good prospects of increasing to many million tons, since the chemical properties of carbamide are responsible for its wide application in the chemical industry in the synthesis of carbamide-aldehyde (first of all, carbamide-formaldehyde) resins widely used as adhesives in the production of wood-fiber plates and furniture production. Urea derivatives are efficient herbicides. Part of the produced carbamide is used to produce melamine. A significant share of it goes to the needs of the pharmaceutical industry.

By its nature, carbamide is a mineral fertilizer that is used on all types of soils for any crops. This type of fertilizer provides a significant increase in crop yields. Compared to other nitrogen fertilizers, carbamide contains the largest amount of nitrogen (46.2%), which mainly determines the economic feasibility of its use as a fertilizer for many crops in any soil. In animal husbandry, urea is added to feed as a protein substitute, and, in the medical practice, it is used as a dehydration agent. The use of carbamide as a nitrogen oxide reducer for cleaning emissions from thermal power plants and waste incineration plants is a new large-scale direction.

To achieve Euro-4 and Euro-5 diesel engine exhaust emission compliance, a urea solution under the trade name AdBlue is used.

In general, with the current volume of urea production of ~ 200 million tons per year, it is possible to utilize up to 150 million tons of CO_2 per year. When assessing the potential of this method of CO_2 utilization, it is important to take into account that 0.58 tons of ammonia is consumed per ton of urea, the ammonia being produced by the very well established but energy- and carbon-intensive Haber–Bosch process [34]. In this regard, research is underway to develop carbon-neutral technologies for producing urea using renewable energy sources. For example, urea was synthesized from nitrogen, carbon dioxide, and water at room temperature in the presence of an electrocatalyst from copper and palladium nanoparticles supported on titanium dioxide (Fig. 5) [35].

2.1.2 Salicylic acid. An important process for using CO_2 as a chemical reagent is the production of salicylic acid by the Kolbe–Schmitt reaction (12):

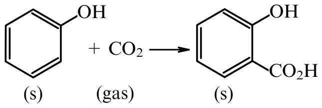

.

This production processes 0.025 million tons of CO_2 annually [22], which is noticeably lower than the volume of its use in the synthesis of urea or polyurethanes.

2.1.3 Methanol. Methanol is a large-capacity product of the chemical industry, used to produce most polymers and a number of organic substances. The worldwide volume of its production is ~ 150 million tons per year. Currently, methanol is mainly produced by catalytic technologies from natural gas and coal gasification products. Hydrogenation of CO_2

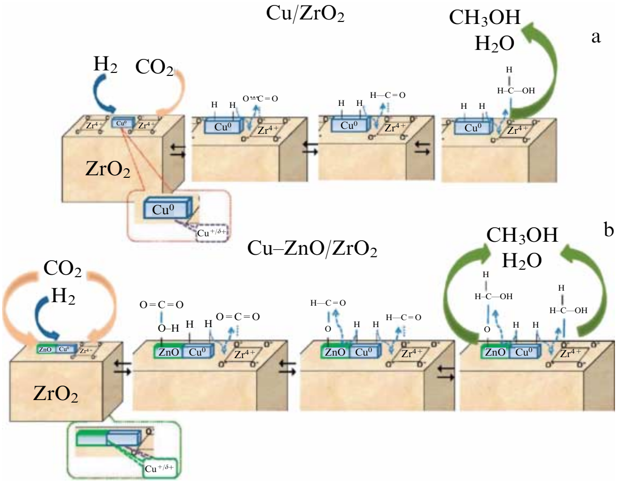

Figure 6. Reaction layout for the production of methanol from CO_2 in the presence of catalysts Cu/ZrO_2 (a) or $Cu–ZnO/ZrO_2$ (b) [38].

according to the reaction (14)

$$\underset{\text{(gas)}}{CO_2} + \underset{\text{(gas)}}{3H_2} \longrightarrow \underset{\text{(l)}}{CH_3OH} + \underset{\text{(l)}}{H_2O}$$

in the presence of catalysts is another way of methanol synthesis, which is one of the most promising chemical processes for the utilization of carbon dioxide [4, 25, 36].

Catalysts based on Cu, Au, Ag, Pd, and Pt, as well as oxide materials $In_2O_3–ZrO_2$, $ZnO–ZrO_2$ [36, 37], are active in the CO_2 hydrogenation reaction. Typically, this process has a carbon dioxide conversion of $\sim$ 20% and a methanol yield of about 10%. In the case of multicomponent catalytic systems, it is believed in [38] that two active centers are involved in the reaction: hydrogen adsorption and dissociation occur on Cu centers, and CO_2 adsorption in the form of bicarbonate occurs on ZrO_2 (Fig. 6). By way of spillover, atomic hydrogen passes from the Cu surface to the ZrO_2 surface, where hydrogenation of adsorbed carbon- and oxygen-containing particles to methanol occurs; the methanol is then desorbed from the surface. The addition of zinc to the composition of the catalyst improves the fineness of copper and provides additional adsorption sites for CO_2. Owing to the optimization of the conditions for the preparation of the catalyst $CuO–ZnO–Al_2O_3/\gamma–Al_2O_3$ and the reaction, the following process parameters were achieved at a temperature of 220 °C and a pressure of 2.8 MPa: methanol yield: 12.8%, CO_2 conversion: 20.3%, methanol selectivity: 63.2% [36].

The use of catalysts based on nitrogen-doped carbon nanotubes (N-CNTs) has been shown to be promising (Fig. 7). It was shown in [39] that, in the case of $Cu–ZrO_2/N$-CNTs, the presence of pyridine nitrogen increases the dispersity and reducibility of the active component, and also provides strong CO_2 adsorption, which leads to an increase in the yield of methanol.

The first modern industrial processing of CO_2 into methanol since 2011 has been carried out by Carbon Recycling International (CRI) in Iceland [4]. The plant's capacity is 4,000 tons of methanol per year. The volume of CO_2 involved in this process is estimated at 6000 tons per year. The hydrogen required for the technology is produced by electrolysis of water using inexpensive and environmentally friendly energy from hydrothermal sources. Another interesting approach and technology for processing carbon dioxide using renewable energy sources, Air to Fuels, was proposed by Canadian Carbon Engineering, which involves the production of carbon-neutral liquid fuels from atmospheric CO_2 and H_2 obtained by electrolysis [40].

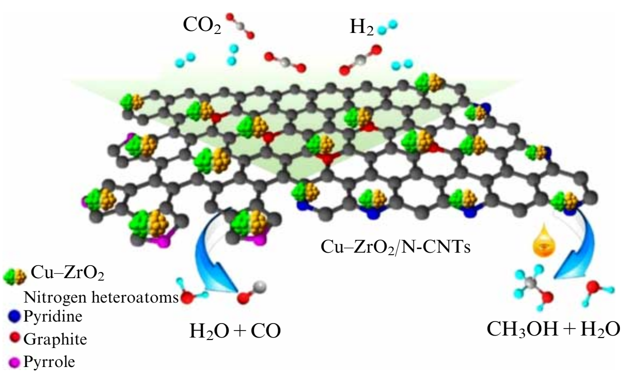

Figure 7. Diagram of the production of methanol by CO_2 hydrogenation in the presence of a $Cu–ZrO_2/N$-CNT catalyst [39].

2.1.4 Formic acid. Formic acid is widely used in agriculture, the textile industry, and medicine. A promising avenue is its use in fuel cells. According to its properties, this compound is suitable for storing chemical energy in renewable energy storage cycles [41]. Formic acid can be obtained by catalytic hydrogenation of CO_2 according to the reaction

$$CO_2 + H_2 \rightarrow HCOOH\,. \tag{15}$$

For the direct catalytic reduction of CO_2 with the production of formic acid, both homogeneous systems — organometallic compounds containing Rh, Ru, and Ir — and heterogeneous systems based on Pt, Pd, Au are used. The efficiency of $Pd/g–C_3N_4$ [42–44], PdNi/CNT–GR [43], and $Ru/Mg_{10}Al_2(OH)_{24}CO_3$ [45] catalysts in reaction (15) has been shown. It has been established that, in the presence of $Pd/g–C_3N_4$, high rates of the process are achieved due to the developed metal–support contact boundary and the participation of the support in the activation of the carbon dioxide molecule [42].

2.1.5 Dimethyl ether. Dimethyl ether (DME) is a reagent in the chemical industry and an alternative type of fuel, which is already actively used in the form of additives to traditional fuels. Synthesis of DME is possible from CO_2 and H_2:

$$2CO_2 + 6H_2 \rightarrow CH_3OCH_3 + 3H_2O\,. \tag{16}$$

The process goes through successive hydrogenation and dehydration reactions, which requires the use of bifunctional catalysts containing metal (often Cu) and acid sites.

It has been shown that reducing the size of Cu-containing active particles is a successful approach to increase the efficiency of this process [41, 46]. However, for industrial applications, further refinement of the formula and structure of the catalysts is needed to achieve higher performance of the process and resistance to deactivation of the catalysts. For example, when using Cu–Fe/HZSM-5 catalysts modified with Ce or La, CO_2 conversion is 18%, DME selectivity is 52% at temperature $T = 260\,°C$ and pressure $P = 3.0$ MPa, the gas hourly space velocity (GHSV) being 1500 ml g^{-1} h^{-1} [46]. Similar process parameters were achieved in the presence of a CO–ZnO–Al_2O_3/γ–Al_2O_3–HZSM-5 catalyst [36]. During a 100-hour experiment at $T = 240$ °C and $P = 2.8$ MPa, a decrease in CO_2 conversion was observed from 26 to 21%, a decrease in DME selectivity from 70 to 56%, and a decrease in DME yield from 18 to 12%.

2.1.6 Methane. The CO_2 methanation reaction (Sabatier process) has recently attracted interest in connection with the search for ways to utilize CO_2 in combination with energy efficient solutions for renewable electricity storage:

$$CO_2 + 4H_2 \rightarrow CH_4 + 2H_2O\,. \tag{17}$$

In this case, it is assumed that a reduction in anthropogenic CO_2 emissions will occur due to the conversion of CO_2 captured from stationary and mobile sources, as well as H_2 produced from renewable energy sources, into CH_4 [47, 48]. The conversion of CO_2 to CH_4 increases with an increase in temperature and a decrease in the CO_2:H_2 ratio in the reactant mixture [48]. The transition metals Ni, Co, Ru, and Rh deposited on various oxide matrices serve as catalysts for this process [49–51]. An increase in low-temperature activity, an improvement in dispersion and reducibility, as well as the resistance to sintering of nickel nanoparticles are the main areas for further improvement of Ni-based catalysts.

An effective approach is the introduction of a second metal (e.g., Fe, Co, Rh, Pt, Pd, and Re). Owing to the formation of the Ni–*M* alloy or complex synergy between two adjacent metal phases, new highly efficient and inexpensive methanation catalysts can be obtained [47]. The study of nickel catalysts supported on perovskite systems (Ni–$La_{0.6}Sr_{0.4}FeO_{3-\delta}$, Ni–$SrTi_{0.7}Fe_{0.3}O_{3-\delta}$) showed that the structural and functional properties of the samples depend on their reducibility [49]. For Ni–$SrTi_{0.7}Fe_{0.3}O_{3-\delta}$, characterized by low reducibility, after activation, there is a slight doping of nickel nanoparticles with iron, which ensures high sample activity. On the contrary, the high reducibility of Ni–$SrTi_{0.7}Fe_{0.3}O_{3-\delta}$ leads to the formation of an NiFe alloy after activation and a decrease in catalytic activity. High performance of the process was achieved in the presence of the Ni–Rh/$LaAlO_3$ catalyst due to a combination of the advantages of a three-dimensional porous support matrix, strong metal–support interaction, and the formation of highly dispersed particles of the NiRh alloy [50]. A process was developed [48] that combines the concentration of CO_2 from the ambient air on the K_2CO_3/Al_2O_3 sorbent, the subsequent desorption of CO_2, and the conversion into methane using an industrial nickel catalyst NKM-2V.

In 2013, Audi launched a Power-to-Gas (PtG) plant in Werlte (northern Germany) for the production of synthetic natural gas from CO_2 and H_2. The plant includes a 6-MW electrolysis plant powered by renewable energy to produce hydrogen and a methanation plant. The scale of carbon dioxide utilization is small — 2800 tons of CO_2 annually [52]. As part of meeting the challenges of moving towards a carbon neutral economy, further optimization of process conditions and a reduction in energy consumption is required.

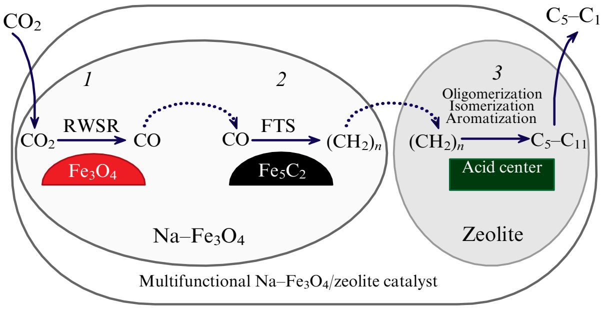

Figure 8. Production of C_5–C_{11} hydrocarbons from CO_2 [53].

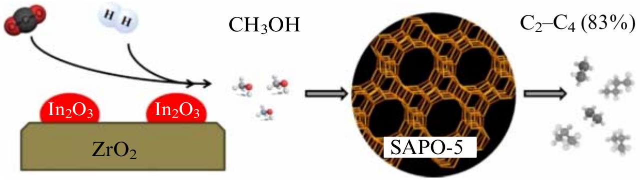

Figure 9. Highly selective conversion of CO_2 into lower hydrocarbons (C_2 – C_4) in the presence of In_2O_3–ZrO_2/SAPO-5 bifunctional catalysts [55].

2.1.7 Synthesis of C_2–C_{11} hydrocarbons. The use of CO_2 in the synthesis of C_2–C_4 hydrocarbons — a modified Fischer–Tropsch process — includes a reaction that is the reverse of the reaction of CO conversion with water vapor,

$$CO_2 + H_2 \rightarrow CO + H_2O\,, \tag{18}$$

and subsequent hydrogenation of CO with the formation of hydrocarbons:

$$nCO + (2n+1)H_2 \rightarrow C_nH_{2n+2} + nH_2O\,, \tag{19}$$

$$nCO + 2nH_2 \rightarrow C_nH_{2n} + nH_2O\,, \tag{20}$$

$$nCO + 2nH_2 \rightarrow C_nH_{2n+2}O + (n-1)H_2O\,. \tag{21}$$

The main disadvantage of this process is the low yield of hydrocarbons (less than 60%) and the formation of large amounts of methane.

The combination of this process with the oligomerization reaction opens up the possibility of utilizing CO_2 and obtaining hydrocarbons of a gasoline fraction containing a mixture of isoparaffins and aromatic and naphthenic hydrocarbons of the C_5–C_{11} composition [53]. The uniqueness of this process consists in the fact that the hydrogenation reaction in the presence of a multifunctional Na–Fe_3O_4/zeolite catalyst occurs in three stages (Fig. 8): (1) CO production by the reverse water shift reaction (RWSR) on Fe_3O_4 centers; (2) hydrogenation of CO to olefins by the Fischer–Tropsch synthesis (FTS) reaction on Fe_5C_2 centers; (3) formation of C_5–C_{11} hydrocarbons as a result of oligomerization, isomerization, and aromatization of olefins on the acid sites of the zeolite. The selectivity for the formation of hydrocarbons is 78% at a CO_2 conversion of 22% [53].

Composite catalysts CuZnZr@Zn–SAPO-34 [54], In_2O_3–ZrO_2/SAPO-5 [55], CuO–ZnO–MnO/SAPO-18 [56] have been developed that combine the function of CO_2 hydrogenation with the formation of methanol and conversion of methanol into light olefins (ethylene, propylene, butylene) (Fig. 9). The low yield of reaction by-products — alkanes — is the main advantage of this process over the

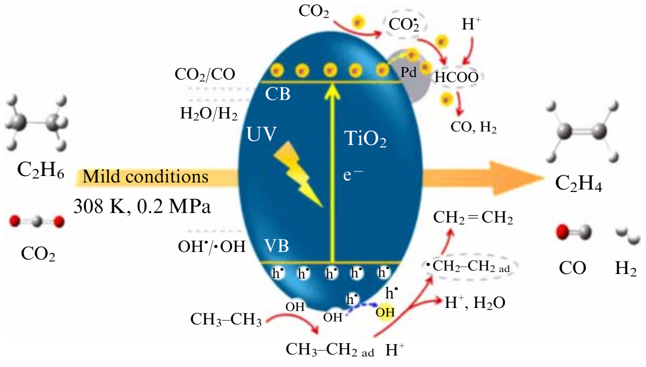

Figure 10. Mechanism of photocatalytic oxidative dehydrogenation of ethane using CO_2 as an oxidant in the presence of a Pd/TiO_2 catalyst [61].

Fischer–Tropsch process. High selectivity for olefins (72%) was achieved in the presence of the CuZnZr@Zn–SAPO-34 catalyst at a ratio of $H_2/CO_2 = 3$, a space velocity of 6000 h^{-1}, a temperature of 400 °C, and a pressure of 2 MPa [54]. This is due to the core-shell structure of the catalyst and the optimum acid–base properties of Zn–SAPO-34. The positive role of Zr in the composition of catalysts was noted, which consists in improving the thermal stability of the material and increasing the concentration of oxygen vacancies, the centers of stabilization of the key intermediate products of the reaction [57].

Another approach to the chemical processing of CO_2 is its use as a mild oxidizer [58–61]. In the oxidative condensation of methane to form ethane and ethylene:

$$CO_2 + 2CH_4 \rightarrow C_2H_6 + CO + H_2O\,, \tag{22}$$

$$CO_2 + 2CH_4 \rightarrow C_2H_4 + 2CO + 2H_2O\,. \tag{23}$$

In the presence of a catalyst ($MnO–SrCO_3$, $ZnO–CeO_2$, or $CaO–CeO_2$), CO_2 conversion is 5–7%, and the yield of C_2 hydrocarbons is up to 5–7% [58, 59].

The reaction of oxidative dehydrogenation of light alkanes with the participation of CO_2,

$$CO_2 + C_2H_6 \rightarrow C_2H_4 + CO + H_2O\,, \tag{24}$$

$$CO_2 + C_3H_8 \rightarrow C_3H_6 + CO + H_2O\,, \tag{25}$$

is carried out at $T = 650-700\,°C$ in the presence of catalysts of various compositions ($Pd/CeZrAlO_x$, $CoMo/CeO_2$, $GaNi/SiO_2$) [60]. The yield of target products (ethylene, propylene) reaches 70%. The use of photocatalytic systems makes it possible to use a renewable energy source and carry out the process under mild conditions (Fig. 10) [61].

2.1.8 Acetic acid. The possibility of obtaining acetic acid from carbon dioxide and methane in the presence of a Cu/M–ZSM-5 catalyst ($M = Li^+$, Na^+, K^+, Ca^{2+}) was shown in [62]. The mechanism of the joint conversion of CO_2 and CH_4 into acetic acid suggests the presence of two types of active sites: metal Cu nanoparticles for the activation of methane and M-containing sites in the cation-exchange positions of the zeolite matrix for the activation of carbon dioxide (Fig. 11). At the first stage, the activation of methane leads CH_4 to the formation of methyl fragments ($-Cu-CH_3$), and the activation of CO_2 leads to the formation of carbonate particles. Furthermore, as a result of the interaction between the intermediates adsorbed on the catalyst surface, acetate fragments ($-Cu-OOCCH_3$) and then acetic acid are formed.

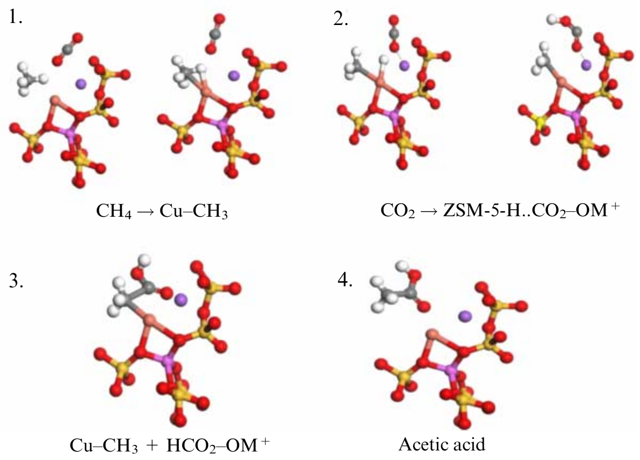

Figure 11. Reaction mechanism of acetic acid formation from methane and CO_2 [62].

2.1.9 Syngas. Carbon dioxide conversion of methane (CDCM) makes it possible to utilize two greenhouse gases and obtain as a product syngas (synthesis gas), suitable in its stoichiometry (1:1) for further conversion into synthetic fuel by the Fischer–Tropsch reaction [63]

$$CO_2 + CH_4 \rightarrow 2CO + 2H_2\,. \tag{26}$$

As in the methanation process, nickel catalysts are highly active in reaction (26) [64, 65]. It has been shown that effective approaches to improve the resistance of nickel systems to deactivation in reforming processes are the use of solid solutions as catalyst precursors [66–68], introduction of promoting additives [69–73], modification of the carrier [74–77], or improvement of the catalyst preparation method [78–80]. It was established in [66] that, in the presence of the catalyst $LaNi_{0.2}Re_xFe_{0.6}O_{3+\delta}–La_3ReO_8$ at $T = 800\,°C$, the conversion of the reagents is more than 90%. The catalyst does not carburize for a long time (70 h), which, according to the authors of [66], is associated with the formation of Ni–Re alloy particles and the implementation of a strong metal–support interaction.

Linde, in collaboration with BASF, has developed the DRYREF^{TM} SMR technology to improve the energy and economic efficiency of steam reforming and carbon dioxide utilization [81]. According to the proposed scheme, CO_2 is added to the reaction mixture containing natural gas and water. As a result, the carbon footprint of syngas production is reduced, steam consumption is reduced, and syngas is obtained with a lower H_2/CO molar ratio than steam reforming of methane.

Carbon dioxide conversion of ethanol makes it possible to obtain syngas from renewable raw materials (CO_2, ethanol):

$$C_2H_5OH + CO_2 \rightarrow 3CO + 3H_2\,. \tag{27}$$

Compared to CDCM, the process is carried out at moderate temperatures and allows high-efficiency utilization of CO_2. In the presence of the $Cu-Ce_{0.8}Zr_{0.2}O_2$ catalyst, complete conversion of ethanol and CO_2 was achieved at a tempera-

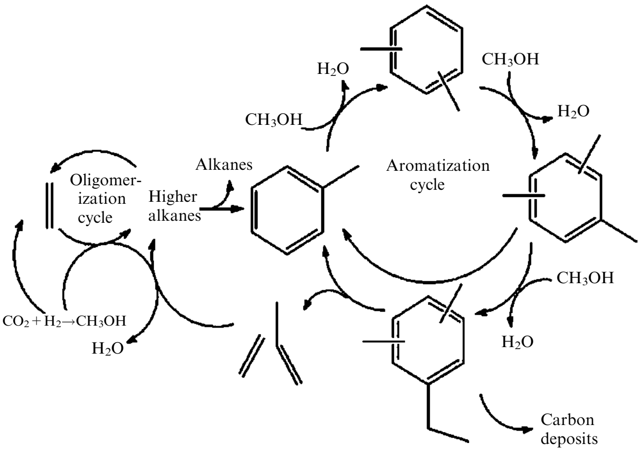

Figure 12. Mechanism of CO_2 aromatization reaction in the presence of a bifunctional catalyst ZnO/ZrO_2–HZSM-5 [84].

ture of 550 °C; at the output, a mixture was obtained with the composition 49% H_2, 41% CO, and 10% CH_4 [82].

2.2 Synthesis of high-molecular-weight organic substances and polymer materials

2.2.1 Aromatic hydrocarbons. One-step synthesis of aromatic hydrocarbons from CO_2 and H_2 occurs on bifunctional ZnZrO/HZSM-5 catalysts with high selectivity for aromatic hydrocarbons (~ 70%), the CO_2 conversion being up to 14% [83, 84]. As shown in Fig. 12, as a result of the catalytic hydrogenation of CO_2 on the ZnZrO component of the catalyst, methanol is formed, which undergoes a chain of transformations into higher alkenes on the zeolite component of the catalyst, ZSM-5. Higher alkenes are involved in further aromatization and methylation reactions (aromatic cycle), forming various aromatic compounds and lower alkenes, which, interacting with methanol, are included in the olefinic cycle. The stability of the catalyst for 100 h and its resistance to carburization were noted, which, in the opinion of the authors, is due to the positive effect of the water formed in the process.

2.2.2 Oxidative dehydrogenation. A promising process will be one using CO_2 for the oxidative dehydrogenation of alkylaromatic hydrocarbons to obtain styrene and its homologues [58]:

$$C_6H_5CH_2CH_3 + CO_2 \rightarrow C_6H_5CHCH_2 + CO + H_2O\,. \tag{28}$$

2.2.3 Synthesis of polymers. An important strategy for using CO_2 is the synthesis of polymers [85–87]. For the synthesis of polyurethanes, polyols and bis-isocyanates are usually used as starting materials [30]. In the traditional Bayer process, the polyol is a polyether derived from fossil fuel-based epoxides such as propylene oxide (Fig. 13). In an alternative process, the polyol is a polycarbonate polyol in which some of the propylene oxide is replaced by carbon from carbon dioxide. The capacity of the plant launched in 2016 by Covestro in Dormagen (Germany) is 5000 tons of polyester carbonate polyol.

With the participation of CO_2 as a reagent, polypropylene carbonate, poly(1,2-glycerol carbonate), and polyurethane have been successfully synthesized. Direct copolymerization of CO_2 with various epoxides (ethylene oxide, propylene oxide, cyclohexene oxide, or isobutylene oxide) creates aliphatic polycarbonates and ether polycarbonates, and these reactions are an efficient way to produce a wide range of biodegradable materials [30]. An optimal method for the preparation of poly(1,2-glycerol carbonate) based on glycerol and CO_2 [86] was revealed, which consists in the copolymerization of ethoxyethyl glycidyl or benzyl glycidyl ether with CO_2 and subsequent removal of the corresponding protective groups by hydrogenation (Fig. 14).

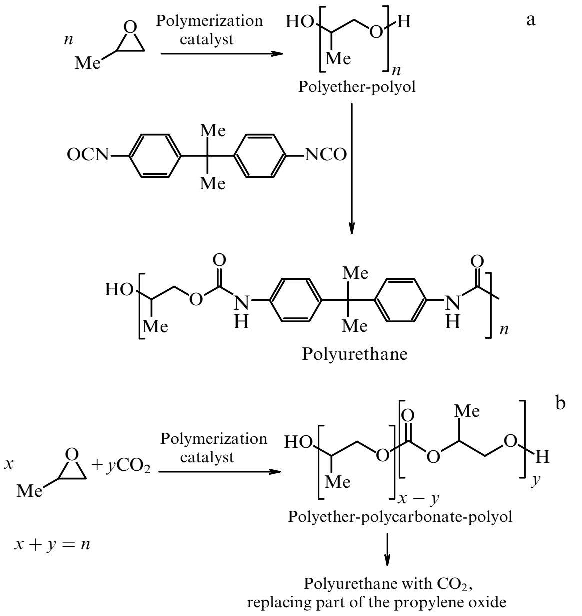

Figure 13. Polyurethane synthesis according to traditional technology (a) and alternative technology with CO_2 utilization (b) [30].

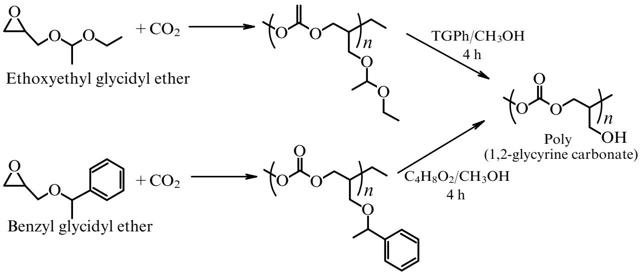

Figure 14. Reaction scheme for the preparation of poly(1,2-glycerol carbonate) using CO_2 as a reagent [86].

In [87], a five-membered cyclocarbonate was synthesized by reacting CO_2 with 1,4-butanediol diglycidyl ether in the presence of a catalyst based on polystyrene resin. At 100% conversion of 1,4-butanediol diglycidyl ether, the cyclocarbonate selectivity was 98.5%. The subsequent chain of syntheses allowed the authors to obtain a new amino alcohol and polyurethane with improved mechanical and thermal properties and solvent resistance.

As part of the implementation of the principles of 'green chemistry' using three-dimensional (3D) printing, an efficient heterogeneous catalyst was developed for the production of propylene carbonate from propylene oxide and CO_2 (Fig. 15) [88]. Synthesis in the presence of a structured CeLaZr catalyst supported on graphene oxide is an alternative to traditional multistage synthesis methods, including the use of homogeneous catalysts and toxic solvents.

In view of the large volumes of polymer production in general, as well as the particularly growing demand for

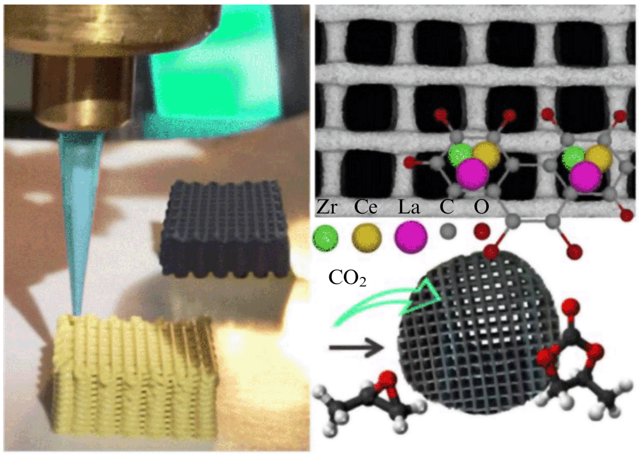

Figure 15. Utilization of CO_2 by the production of propylene carbonate in the presence of a CeZrLa/graphene nanocatalyst obtained using a 3D printer [88].

biodegradable materials, the development of this CO_2 utilization technology is the most important area in the production of multi-purpose polymers. According to [2], by 2050, the volume of carbon dioxide processing into polymer products will be 10–50 million tons per year.

2.3 Combined steam and carbon dioxide conversion of methane

Steam-carbon dioxide reforming of methane (29) is a unique environmentally friendly process that allows you to simultaneously utilize three greenhouse gases (carbon dioxide, methane, water vapor):

$$2CH_4 + CO_2 + H_2O \leftrightarrow 3CO + 5H_2\,. \qquad (29)$$

A comparative thermodynamic analysis of three reforming processes (Fig. 16) showed that an increase in the reaction temperature leads to an increase in the conversion of the initial reagents and an increase in the yield of the target products: hydrogen and carbon monoxide. In contrast to purely steam reforming of methane, steam-carbon dioxide reforming ensures the production of hydrogen-containing gas with the utilization of all components, and CO_2 emission is completely eliminated. By varying the molar ratio of $CH_4:CO_2:H_2O$, the H_2/CO values are flexibly regulated over a wide range (1–3). A directional change in the O/C ratio can optimize the process parameters, ensuring a given completeness of the conversion of the reagents and avoiding the formation of reaction by-products [89–91]. The presence of water vapor in the reaction mixture expands the region of system resistance to the formation of carbonaceous deposits (Fig. 16).

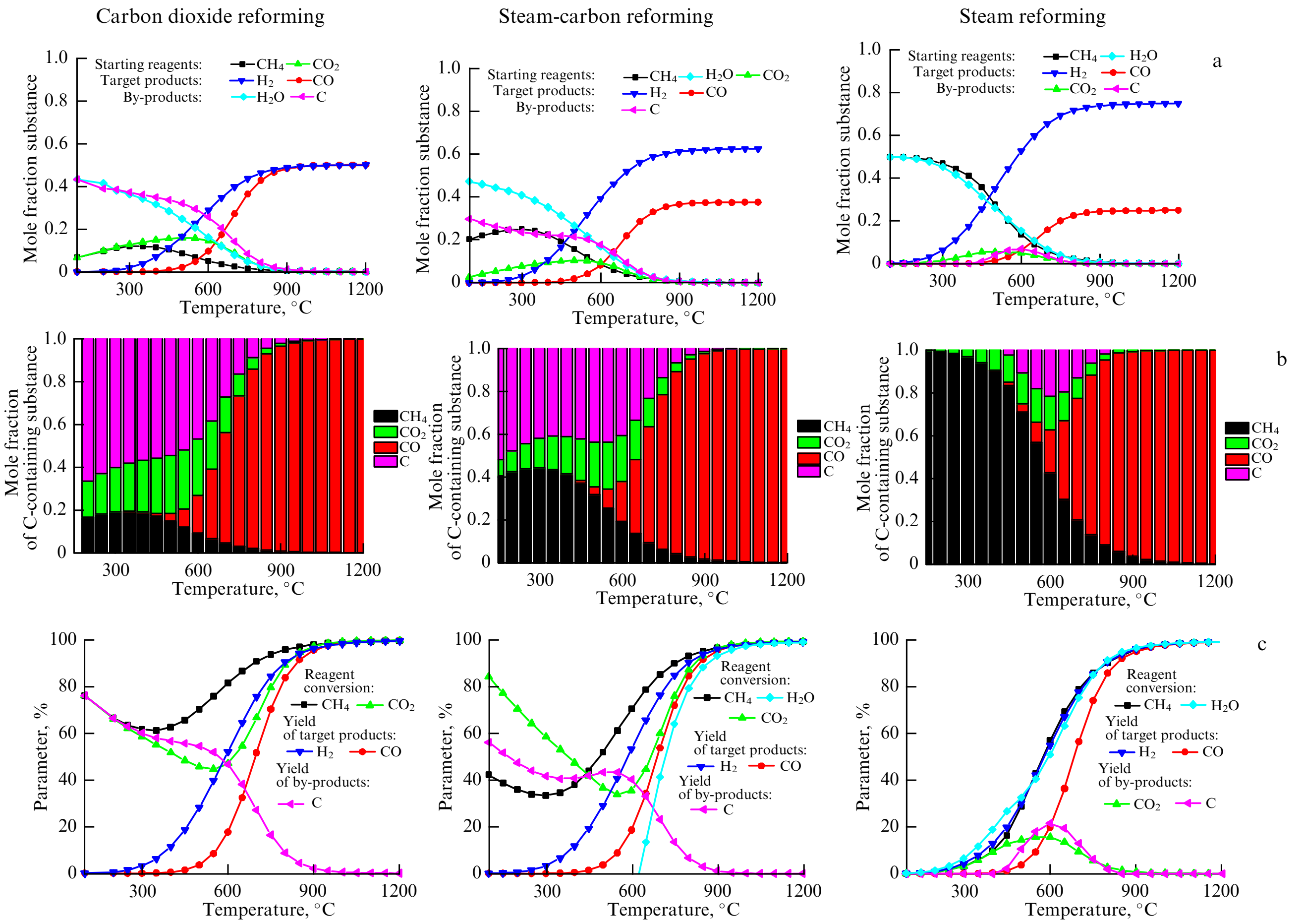

Figure 16. Thermodynamic analysis of reactions of carbon dioxide ($CH_4:CO_2 = 1:1$), steam-carbon dioxide ($CH_4:CO_2:H_2O = 1:0.5:0.5$), and steam ($CH_4:H_2O = 1:1$) methane reforming: mole fraction of substances (a), mole fraction of C-containing substances (b), and process parameters (c). Equilibrium compositions were determined using the IVTANTHERMO program by minimizing the Gibbs free energy.

Table 4. Chemical composition and textural and structural characteristics of precursors of nickel catalysts for steam-carbon dioxide reforming of methane.

Sample	Chemical composition, wt %				Textural characteristics*			Phase composition (CSR**/cell parameter, nm)	
	Ce	La	Mg	Ni	$S_{\rm BET}$, $\rm m^2\ g^{-1}$	V_Σ, $\rm cm^3\ g^{-1}$	$D_{\rm pore}$, nm	Before activation	After activation
CeO_2 support	82.6	—	—	—	74	0.16	8.5	CeO_2 (11.0/0.5412)	
$Ce_{0.8}Ni_{0.2}O_{1.8}$	72.1	—	—	11.0	105	0.23	8.8	CeO_2 (5.5/0.5412)	CeO_2 (25.0/0.5419) Ni (15.0)
$(Ce_{0.8}La_{0.2})_{0.8}Ni_{0.2}O_{1.7}$	57.8	14.7	—	9.8	100	0.31	12.3	CeO_2***(6.0/0.5468)	
$(Ce_{0.5}La_{0.5})_{0.8}Ni_{0.2}O_{1.6}$	37.5	36.9	—	9.4	50	0.18	15.6	CeO_2*** (4.0/0.5553)	CeO_2 (22.0/0.5600) Ni (12.0)
$(Ce_{0.2}La_{0.8})_{0.8}Ni_{0.2}O_{1.4}$	17.6	58.8	—	9.2	35	0.15	18.1	CeO_2*** (4.0/0.5661)	
$La_{0.8}Ni_{0.2}O_{1.4}$	—	74.2	—	10.0	25	0.10	17.1	$La_2O_2CO_3$	
$(Ce_{0.8}Mg_{0.2})_{0.8}Ni_{0.2}O_{1.6}$	69.2	—	3.5	9.9	93	0.25	10.8	CeO_2*** (5.5/0.5408), MgO – NiO (4.0/0.4182)	
$(Ce_{0.5}Mg_{0.5})_{0.8}Ni_{0.2}O_{1.4}$	57.4	—	9.0	9.2	36	0.15	17.0	CeO_2*** (3.5/0.5410), MgO – NiO (3.6/0.4204)	CeO_2 (19.0/0.5413) MgO (13.0/4.215) Ni (13.0)
$(Ce_{0.2}Mg_{0.8})_{0.8}Ni_{0.2}O_{1.2}$	36.3	—	21.2	9.7	23	0.10	17.7	CeO_2*** (5.5/0.5414), MgO – NiO (8.5/0.4212)	
$Mg_{0.9}Ni_{0.1}O_{1.5}$	—	—	54.1	10.2	23	0.12	20.3	MgO – NiO (18.0/0.4222)	

* $S_{\rm BET}$ — Brunauer–Emmett–Teller (BET) specific surface area, V_Σ — total pore volume, $D_{\rm pore}$ — average pore diameter.

** CSR — coherent scattering region.

*** Diffraction pattern of a CeO_2-like phase.

In Iran, the production of methanol is 3030 tons per day based on the process of steam-carbon dioxide conversion of natural gas with a capacity of 86,000 $\rm nm^3\ h^{-1}$ [92]. In Japan, a plant for the production of synthetic liquid hydrocarbons with a capacity of 7 barrels per day was launched based on steam-carbon dioxide reforming of methane and testing the catalyst and the JNOC (Japan National Oil Corporation) process [93]. The catalyst is a ring with an outer diameter of 16 mm, an inner diameter of 8 mm, and a height of 16 mm. The process is carried out at a temperature of 890 °C, a pressure of 2 MPa, and a space velocity of 3000 $\rm h^{-1}$. The resulting syngas is H_2/CO balanced for Fischer–Tropsch synthesis, as well as for the production of methanol and dimethyl ether. This technology is considered to be effective in small natural gas fields with a high CO_2 content, as well as in the processing of off-gases containing a high concentration of CO_2 in gas processing plants and the production of liquefied natural gas. A catalyst for the process of steam-carbon dioxide reforming [94] based on noble metals supported on MgO was developed.

Nickel-containing catalysts, due to their availability, low cost, and high performance, in contrast to expensive catalysts based on noble metals, seem to be suitable for use in hydrocarbon feedstock reforming processes [95–97]. However, under the conditions of a catalytic process, due to the influence of the reaction medium, deactivation of nickel-containing catalysts is possible because of the formation of carbon deposits, sintering, and phase transformations. Stabilization of highly dispersed nickel particles by selecting the support matrix makes it possible to increase their resistance to carburization [98–101]. As supports, of particular interest are Ce-containing oxide systems, which are distinguished by the stability of the fluorite-type cubic structure upon varying their chemical composition, which have unique redox properties, high oxygen capacity, and oxygen mobility of the crystal lattice [102–104].

To implement a strong metal–support interaction, the formation of nanoparticles of the active component, and a developed metal-oxide interfacial surface, an approach based on *in situ* formation of catalytically active particles by activating complex oxides in a reducing or reaction medium has proven itself [67, 68, 105, 106]. Precursors are compounds in which the cations of the active component and the support cations form a joint phase, for example, layered double hydroxides $[Mg_{1-x-y}Ni_xAl_y(OH)_2](CO_3)_{y/2}\times\ mH_2O$ [107, 108], oxides with the structure of fluorite $Ce_{1-x}Ni_xO_y$ [67, 109], perovskite $LaNiO_3$ [70, 106, 110], and spinel $(Ni_{0.75}Mg_{0.25})Al_2O_4$ [111].

Directed thermal activation of complex oxides/hydroxides leads to the destruction of the structure, nucleation, growth, and the formation of metal particles and clusters stabilized on the oxide surface of the support. In accordance with this approach, complex oxides $(Ce_{1-x}M_x)_{0.8}Ni_{0.2}O_y$ (M = La, Mg; $x = 0, 0.2, 0.5, 0.8, 1$; $1.0 \leqslant y \leqslant 1.8$) prepared by the ester polymer precursor method were used (Table 4). The study of the genesis and textural and structural properties of $(Ce_{1-x}M_x)_{0.8}Ni_{0.2}O_y$ showed [105] that, after calcination at $T = 500\,°C$ in an oxidizing environment, $(Ce_{1-x}M_x)_{0.8}Ni_{0.2}O_y$ are mesoporous materials, which are substitutional solid solutions with a fluorite-type cubic structure with deposited particles of the Ni-containing phase. The oxides are characterized by a high defectiveness of the structure and a crystallite size of less than 4 nm. In the case of M = La, the Ni cations are mainly stabilized in the composition of the Ce–La–Ni–O-solid solution, and for M = Mg, in the composition of highly dispersed particles of

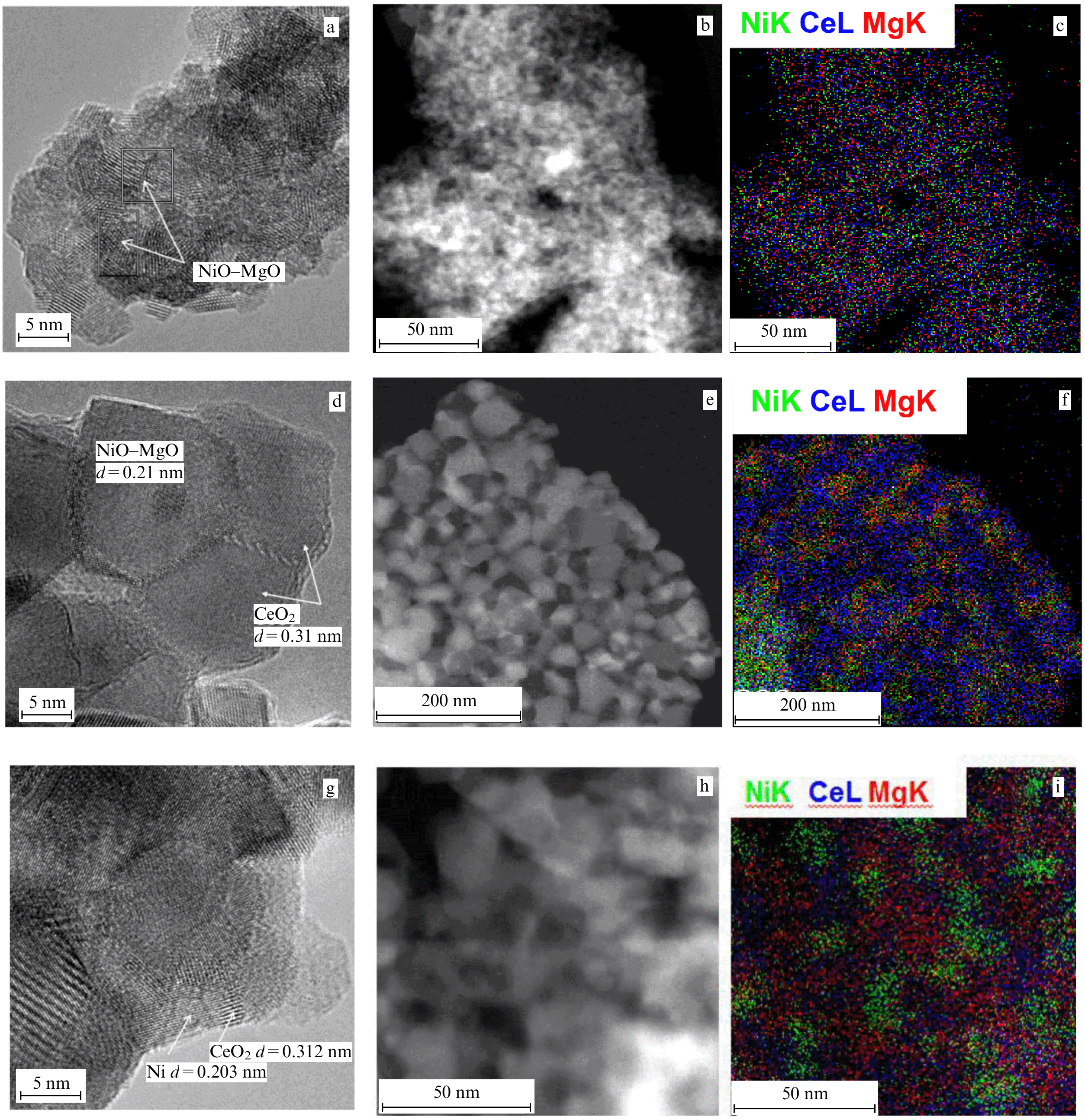

Figure 17. Pictures of sections of material $(Ce_{0.5}Mg_{0.5})_{0.8}Ni_{0.2}O_{1.4}$ after treatment in air at 500 °C (a–c), in air at 800 °C (d–f), and in a reducing medium at 800 °C (g–i), obtained using transmission electron microscopy (TEM) (a, d, g), dark-field scanning TEM with registration of high-angle scattered electrons (b, e, h). Mapping by energy dispersive X-ray (EDX) spectroscopy showing distribution of elements after treatment in an oxidizing environment at $T = 500$ °C (c), an oxidizing environment at $T = 800$ °C (e), and a reducing environment at $T = 800$ °C (i) [105].

the NiO–MgO solid solution. After thermal treatment at $T = 800$ °C in an oxidizing medium, a two-phase system is observed, including CeO_2 and a solid solution of NiO–MgO, and in a reducing medium, highly dispersed NiO particles with a size of 5–10 nm are formed (Fig. 17). Metal particles are defective, have a polycrystalline structure, and are easily reoxidized in air to form 'core@shell' Ni@NiO structures [105].

The presence of a high specific surface in the obtained samples, a high concentration of oxygen vacancies, and a highly dispersed state of NiO particles deposited on the surface of the oxide matrix provided unique functional properties of the developed materials in catalysis [67, 68]. It was determined (Table 5) that for the implementation of effective steam-carbon dioxide reforming of methane and resistance to carburization, it is necessary to use: (1) the method of ester polymer precursors; (2) activation in a reducing environment; (3) a Ce–Mg–O-containing oxide matrix.

We have developed a catalyst resistant to carburization with the optimal composition $(Ce_{0.8}Mg_{0.2})_{0.8}Ni_{0.2}O_{1.4}$, which ensures stable parameters of the steam-carbon dioxide conversion of methane — the yield of target products is more than 90% with a conversion of reagents of at least 85% at $T = 800$ °C (Fig. 18), which is close to the equilibrium values. The results obtained are comparable to or exceed those described in the literature [112], which indicates that the

Table 5. Indicators of the steam-carbon dioxide conversion of methane at $T = 750\,^{\circ}\mathrm{C}$ in the presence of Ni catalysts: optimization of the catalyst composition, preparation, and activation method.

Sample*	Processing conditions	CH_4 conversion, %	CO_2 conversion, %	H_2 yield, %	CO yield, %	H_2/CO	Content of carbonaceous deposits, wt %
Ni/CeO_2 (P)	H_2 800 °C	68	80	64	69	1.2	21.6
$Ce_{0.8}Ni_{0.2}O_{1.8}$ (C)		61	63	66	66	1.4	2.7
$Ni/Ce_{0.5}La_{0.5}O_{1.75}$ (P)		76	82	80	76	1.4	26.7
$(Ce_{0.5}La_{0.5})_{0.8}Ni_{0.2}O_{1.6}$ (C)		74	83	61	69	1.1	8.0
$Ni/Ce_{0.5}Mg_{0.5}O_{1.5}$ (P)		82	69	91	82	1.6	1.9
$(Ce_{0.5}Mg_{0.5})_{0.8}Ni_{0.2}O_{1.4}$ (C)		92	83	93	91	1.5	0.9
	O_2 800 °C	59	50	70	57	1.6	No data
	Ar 800 °C	39	45	46	47	14	No data

*P — incipient wetness impregnation method, C — method of ester polymer precursors.

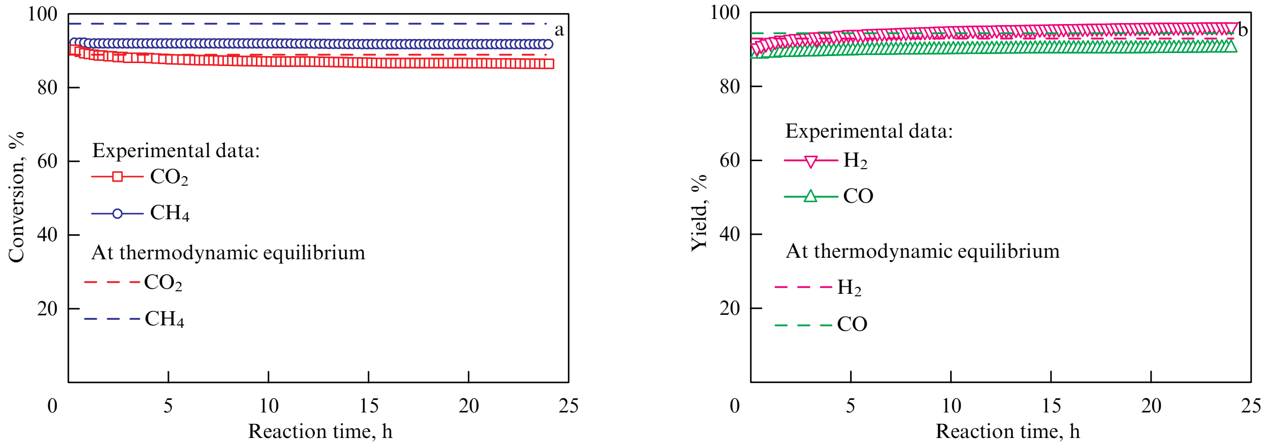

Figure 18. Conversion of carbon dioxide and methane (a), yield of hydrogen and CO (b) in steam-carbon dioxide conversion of methane at a temperature of 800 °C in the presence of a catalyst $(Ce_{0.8}Mg_{0.2})_{0.8}Ni_{0.2}O_{1.6}$.

use of the developed catalysts for the efficient conversion of carbon dioxide into valuable chemical products is promising.

3. Conclusion

We are currently facing a scenario in which the effects of global warming are rapidly intensifying and the search for solutions is beyond a mere technological challenge. More integrated solutions are needed that connect different areas and thus bring about a change in the way of life, thereby guaranteeing the future of the planet and the sustainable development of society.

These new approaches have led, for instance, to the fact that one of the main greenhouse gases, CO_2, is no longer considered to be waste, but a raw material from which a significant range of value-added products can be obtained. This idea explains the renewed interest in CO_2 conversion reactions, which to date have been used in industry only to process relatively small amounts of it. Currently, there is no large-scale production that would allow industrial processes to be carried out without CO_2 emissions, because the economic viability of CO_2 processing reactions in most cases also largely depends on a sustainable supply of H_2.

To curb global warming and climate change in accordance with a national strategy for the transition to a carbon-neutral economy, the development and improvement of sorption and catalytic technologies for CO_2 utilization are relevant. This will not only reduce CO_2 emissions but also reduce society's dependence on nonrenewable fossil fuels.

The use of carbon dioxide as a building block for the synthesis of chemicals is the basis for the sustainable development of the chemical industry and an effective approach to minimizing the carbon footprint. CO_2 is a nontoxic, cheap, accessible, renewable reagent, but its activation requires a significant amount of energy due to the high stability of the molecule. The solution to the problem is the development of catalysts capable of activating the CO_2 molecule efficiently and selectively. Chemical methods of CO_2 utilization include endothermic reactions for the synthesis of low molecular weight compounds (HCOOH, CO, H_2CO, CH_3OH) and exothermic reactions for the preparation of high molecular weight organic substances that are widely in demand on the market (carbamates RR′NCOOR″, carbonates $(RO)_2CO$, carboxylates RCOOH) which, on the other hand, can act as energy carrier molecules in renewable energy storage cycles.

The chemical reactions and heterogeneous catalysts used to convert CO_2 into valuable chemicals such as urea, methanol, polyurethanes, CO, CH_4, and C_2H_4 have been discussed in this article. The CO_2 molecule is thermodynamically very stable, its activation requires a great deal of energy, and the production of this energy is sometimes accompanied by the emission of CO_2. Therefore, to achieve the overall effect of reducing CO_2 emissions, it is necessary to develop new efficient catalysts for CO_2 conversion. The catalytic conversion of CO_2 can occur in the gas or liquid phase, in electrochemical cells. Since the solubility of CO_2 is rather low in an aqueous solution, the conversion of CO_2 in the liquid phase is usually slow. In this review, we mainly considered processes in the gas phase, in which catalysts were involved: metal oxides, supported metals, carbides, and carbon materials.

The use of homogeneous catalysts in the production of formic acid is still limited due to the low solubility of CO_2, and the development of an active heterogeneous catalyst for this process has very good prospects.

Processes using heat and light as energy sources will undoubtedly be in demand in order to minimize overall energy consumption. Electrochemical conversion of CO_2 using catalysts is still at an early stage and has significant potential for further optimization.

Steam-carbon dioxide reforming of methane is an environmentally friendly process that allows the simultaneous use of three greenhouse gases (carbon dioxide, methane, and water vapor) and obtaining synthesis gas of optimal composition. We have developed methods for designing catalytic systems for the steam-carbon dioxide conversion of methane, including the *in situ* formation of catalytically active particles.

The development of technologies for the catalytic conversion of CO_2 into valuable chemical products and the gradual development by the industry of the production of a dozen value-added products are making a high-tech contribution to reducing CO_2 emissions. At present, this contribution, which is still quite modest, amounts to about 1% of global emissions, but the prospects are very attractive. In our opinion, in the future, the gradual processing of CO_2, previously postponed at the stage of carbon capture and storage (CCS), should be considered one of the methods of catalytic technologies. This will be a new incremental step in the Atmospheric Carbon Dioxide Reduction (carbon utilization and storage, CUS) strategy.

Acknowledgment. The authors express their gratitude to the Russian Foundation for Basic Research and the State Foundation for Natural Sciences of China for the financial support (project no. 20-53-53018).

References

1. Arutyunov V S *Neft' XXI. Mify i Real'nost' Al'ternativnoi Energetiki* (Oil XXI. Myths and Reality of Alternative Energy) (Moscow: Algoritm, 2016)
2. Hepburn C et al. *Nature* **575** 87 (2019)
3. Mikkelsen M, Jørgensen M, Krebs F C *Energy Environ. Sci.* **3** 43 (2010)
4. Goeppert A et al. *Chem. Soc. Rev.* **43** 7995 (2014)
5. Erneuerbare-Energien-und-Klimaschutz.de, Specific Carbon Dioxide Emissions of Various Fuels, Specif. Carbon Dioxide Emiss. Var. Fuels. (2015) (accessed 15 May 2019), https://www.volker-quaschning.de/datserv/CO_2-spez/index_e.php
6. Makarov A A, Mitrova T A, Kulagin V A (Eds) *Prognoz Razvitiya Energetiki Mira i Rossii* (Forecast of the Development of the Energy Industry in the World and Russia) (Moscow: INEI RAN, Moskovskaya Shkola Upravleniya SKOLKOVO, 2019)
7. Khokhlov A, Melnikov Yu *Ugol'naya Generatsiya*: *Novye Vyzovy i Vozmozhnosti* (Coal Generation: New Challenges and Opportunities) (Moscow: Tsentr Energetiki MShU SKOLKOVO, 2019); Electronic resource (accessed 21 April 2021), https://energy.skolkovo.ru/downloads/documents/SEneC/Research/SKOLKOVO_EneC_Coal_generation_ 2019.01.01_Rus.pdf
8. Russell A T, in *Air Pollution and Cancer* (IARC Scientific Publ., No. 161, Eds K Straif, A Cohen, J Samet) (Lyon: Intern. Agency for Research on Cancer, 2013) p. 37
9. Engineering ToolBox. Combustion of Fuels — Carbon Dioxide Emission, Electronic resource (accessed 11 March 2021), https://www.engineeringtoolbox.com/co2-emission-fuels-d_1085.html%0A; http://www.engineeringtoolbox.com/co2-emission-fuels-d_1085.html
10. Gimani G et al. *Energ. Byull.* (72) (2019)
11. Smirnov B M *High Temp.* **57** 573 (2019); *Teplofiz. Vys. Temp.* **57** 609 (2019)
12. Archer D *Global Warming. Understanding the Forecast* (Hoboken, NJ: John Wiley and Sons, 2011)
13. Yang H et al. *J. Environ. Sci.* **20** 14 (2008)
14. Alper E, Orhan O Y *Petroleum* **3** 109 (2017)
15. *Energoeffektivnaya Rossiya* (Energy Efficient Russia) (McKinsey and Co., 2009)
16. Olajire A A *J. Petroleum Sci. Eng.* **109** 364 (2013)
17. Qin A et al. *ACS Sustain. Chem. Eng.* **7** 4523 (2019)
18. Zhang Y et al. *J. Mater. Chem. A* **7** 7962 (2019)
19. Sun Y et al. *J. Mater. Chem. A* **6** 23587 (2018)
20. Zhao H et al. *J.* CO_2 *Util.* **44** 101415 (2021)
21. Wang Q et al. *Energy Environ. Sci.* **4** 42 (2011)
22. Bazzanella A, Krämer D *Technologies for Sustainability and Climate Protection — Chemical Processes and Use of* CO_2 (Frankfurt: DECHEMA Gesellschaft für Chemische Technik und Biotechnologie e.V., 2019)
23. Heltzel J M *Chem. Commun.* **54** 6184 (2018)
24. Bobbink F D, Van Muyden A P, Dyson P J *Chem. Commun.* **55** 1360 (2019)
25. Ho H J, Iizuka A, Shibata E *Ind. Eng. Chem. Res.* **58** 8941 (2019)
26. Sels B, Van de Voorde M *Applications in the Chemical Industry, Energy Development, and Environment Protection* (Weinheim: Wiley-VCH Verlag GmbH and Co, 2017)
27. He M, Sun Y, Han B *Angew. Chem. Int. Ed.* **52** 9620 (2013)
28. de Falco M, Iaquaniello G, Centi G CO_2: *A Valuable Source of Carbon* (London: Springer, 2013)
29. Aresta M, Dibenedetto A, Angelini A *Chem. Rev.* **114** 1709 (2014)
30. North M, Styring P *Faraday Discuss.* **183** 489 (2015)
31. Gazokhimicheskii zavod. Proizvodstvo karbamida (Gas chemical plant. Carbamide production). Electronic resource (accessed 21 April 2021), https://salavat-neftekhim.gazprom.ru/about/working/applying/
32. 'Akron' zapustil novyi agregat po proizvodstvu karbamida (Akron launched a new carbamide production unit). Electronic resource. (assesses 21 April 2021), https://53news.ru/novosti/44364-akron-zapustil-novyj-agregat-po-proizvodstvu-karbamida.html
33. 'Akron' aktiviziruyet raboty po proektu 'Karbamid 6+' (Akron intensifies work on the Urea 6+ project), Electronic resource (accessed 21 April 2021), http://rccnews.ru/news/fertilizers/104661/
34. Jarvis S M, Samsatli S *Renew. Sustain. Energy Rev.* **85** 46 (2018)
35. Chen C et al. *Nat. Chem.* **12** 46 (2020)
36. Ren S et al. *Fuel* **239** 1125 (2019)
37. Dang S et al. *Catal. Today* **330** 61 (2019)
38. Arena F et al. *Appl. Catal. A Gen.* **350** 16 (2008)
39. Sun Y et al. *Catal. Today* **307** 212 (2018)
40. AIR TO FUELSTM PLANTS, Electronic resource (accessed 21 April 2021), https://carbonengineering.com/our-technology
41. Yan N, Philippot K *Curr. Opin. Chem. Eng.* **20** 86 (2018)
42. Park H *Chem. Commun.* **52** 14302 (2016)
43. Nguyen L T M et al. *RSC Adv.* **5** 105560 (2015)
44. Lee J H et al. *J. Mater. Chem. A* **2** 9490 (2014)
45. Mori K, Taga T, Yamashita H *ACS Catal.* **7** 3147 (2017)
46. Qin Z Z et al. *Catal. Commun.* **75** 78 (2016)

47. Tsiotsias A I et al. *Nanomaterials* **11** 28 (2021)
48. Veselovskaya J V, Parunin P D, Okunev A G *Catal. Today* **298** 177 (2017)
49. Thalinger R et al. *J. Catal.* **337** 26 (2016)
50. Arandiyan H et al. *ACS Appl. Mater. Interfaces* **10** 16352 (2018)
51. Golosman E Z, Efremov, V N *Catal. Ind.* **4** 267 (2012); *Kataliz Promyshl.* **5** 36 (2012)
52. Audi opens power-to-gas facility in Werlte/Emsland; e-gas from water, green electricity and CO_2, Electronic resource (accessed 11 March 2021), https://www.greencarcongress.com/2013/06/audi-20130625.html
53. Wei J et al. *Nat. Commun.* **8** 15174 (2017)
54. Chen J et al. *Fuel* **239** 44 (2019)
55. Wang J *J.* CO_2 *Util.* **27** 81 (2018)
56. Ateka A et al. *Fuel Process. Technol.* **181** 233 (2018)
57. Dang S et al. *J. Catal.* **364** 382 (2018)
58. Rahman S T et al. *Catalysts* **10** 1 (2020)
59. Cai X, Hu Y H *Energy Sci. Eng.* **7** 4 (2019)
60. Li G et al. *Green Chem.* **23** 689 (2021)
61. Zhang R et al. *ACS Catal.* **8** 9280 (2018)
62. Rabie A M, Betiha M A, Park S E *Appl. Catal. B Environ.* **215** 50 (2017)
63. Nedolivko V V et al. *Russ. J. Appl. Chem.* **93** 765 (2020); *Zh. Prikladn. Khim.* **93** 763 (2020)
64. Jang W J et al. *Catal. Today* **324** 15 (2019)
65. Krylov O V *Ros. Khim. Zh.* **44** 19 (2020)
66. Zubenko D, Singh S, Rosen B A *Appl. Catal. B* **209** 711 (2017)
67. Matus E V et al. *Kinet. Catal.* **60** 221 (2019); *Kinetika Kataliz* **60** 245 (2019)
68. Matus E V et al. *Kinet. Catal.* **60** 496 (2019); *Kinetika Kataliz* **60** 532 (2019)
69. Matus E B *Int. J. Hydrogen Energy* **45** 33352 (2020)
70. Ismagilov I Z et al. *Appl. Catal. A* **481** 104 (2014)
71. Kerzhentsev M A et al. *Kinet. Catal.* **58** 601 (2017); *Kinetika Kataliz* **58** 614 (2017)
72. Ligthart D A J M, Pieterse J A Z, Hensen E J M *Appl. Catal. A* **405** 108 (2011)
73. Hou Z et al. *Appl. Surf. Sci.* **233** 58 (2004)
74. Ismagilov I Z et al. *Kinet. Catal.* **56** 397 (2015); *Kinetika Kataliz* **56** 394 (2015)
75. Matus E V et al. *Kinet. Catal.* **58** 610 (2017); *Kinetika Kataliz* **58** 623 (2017)
76. Ismagilov I Z at al. *Int. J. Hydrogen Energy* **39** 20992 (2014)
77. de Abreu A J, Lucrédio A F, Assaf E M *Fuel Process. Technol.* **102** 140 (2012)
78. Matus E V et al. *J. Nanoparticle Res.* **21** 11 (2019)
79. Ismagilov I Z *Eurasian Chem. J.* **19** 3 (2017)
80. Zhang L et al. *J. Mol. Catal. A* **297** 26 (2009)
81. Smaller carbon footprint. Higher process efficiency, Electronic resource (accessed 21 April 2021), https://www.engineering.linde.com/dryref
82. Chen Q et al. *J. Saudi Chem. Soc.* **23** 111 (2019)
83. Li Z et al. *Joule* **3** 570 (2019)
84. Zhang X et al. *J.* CO_2 *Util.* **29** 140 (2019)
85. Ye S et al. *Adv. Ind. Eng. Polym. Res.* **2** 143 (2019)
86. Geschwind J, Frey H *Macromolecules* **46** 3280 (2013)
87. Li X et al. *J.* CO_2 *Util.* **26** 52 (2018)
88. Middelkoop V et al. *J. Clean. Prod.* **214** 606 (2019)
89. Matus et al. *J. Phys. Conf. Ser.* **1749** 012023 (2021)
90. Pashchenko D *Int. J. Energy Res.* **44** 438 (2020)
91. Singh S et al. *Int. J. Hydrogen Energy.* **43** 17230 (2018)
92. Rostrup-Nielsen J R, Sehested J, Noerskov J K *Adv. Catal.* **47** 65 (2002)
93. Yagi F et al. *Stud. Surf. Sci. Catal.* **147** 127 (2004)
94. Yagi F et al. *Catal. Today* **104** (1) 2 (2005)
95. Usachev N Ya et al. *Ros. Khim. Zh.* **52** 22 (2008)
96. De S et al. *Energy Environ. Sci.* **9** 3314 (2016)
97. Horn R, Schlögl R *Catal. Lett.* **145** 23 (2015)
98. Ismagilov Z R et al. *Catal. Today* **323** 166 (2019)
99. Aramouni N A K et al. *Energy Convers. Manag.* **150** 614 (2017)
100. Sehested J, Gelten J A P, Helveg S *Appl. Catal. A* **309** 237 (2006)
101. Bengaard H S et al. *J. Catal.* **209** 265 (2002)
102. Mullins D R *Surf. Sci. Rep.* **70** 42 (2015)
103. Rodriguez J A et al. *Chem. Soc. Rev.* **46** 1824 (2017)
104. Bruix A, Neyman K M *Catal. Lett.* **146** 2053 (2016)
105. Matus E V et al. *J. Struct. Chem.* **61** 1080 (2020); *Zh. Strukt. Khim.* **61** 1143 (2020)
106. Kim J H et al. *ACS Nano* **15** 81 (2021)
107. Li D et al. *Int. J. Hydrogen Energy* **39** 10959 (2014)
108. Hernández W Y et al. *Green Chem.* **19** 5269 (2017)
109. Fuentes R O et al. *RSC Adv.* **6** 64861 (2016)
110. Kwon O et al. *J. Phys. Energy* **2** 032001 (2020)
111. Misture S T et al. *Catal. Sci. Technol.* **5** 4565 (2015)
112. Jabbour K *J. Energy Chem.* **48** 54 (2020)